

Improving Dynamic Object Interactions in Text-to-Video Generation with AI Feedback

Hiroki Furuta^{1,2,*}, Heiga Zen¹, Dale Schuurmans¹, Aleksandra Faust¹, Yutaka Matsuo², Percy Liang³ and Sherry Yang¹

¹Google DeepMind, ²The University of Tokyo, ³Stanford University, *Work done as Student Researcher at Google DeepMind.

Large text-to-video models hold immense potential for a wide range of downstream applications. However, these models struggle to accurately depict dynamic object interactions, often resulting in unrealistic movements and frequent violations of real-world physics. One solution inspired by large language models is to align generated outputs with desired outcomes using external feedback. This enables the model to refine its responses autonomously, eliminating extensive manual data collection. In this work, we investigate the use of feedback to enhance the object dynamics in text-to-video models. We aim to answer a critical question: what types of feedback, paired with which specific self-improvement algorithms, can most effectively improve text-video alignment and realistic object interactions? We begin by deriving a unified probabilistic objective for offline RL finetuning of text-to-video models. This perspective highlights how design elements in existing algorithms like KL regularization and policy projection emerge as specific choices within a unified framework. We then use derived methods to optimize a set of text-video alignment metrics (e.g., CLIP scores, optical flow), but notice that they often fail to align with human perceptions of generation quality. To address this limitation, we propose leveraging vision-language models to provide more nuanced feedback specifically tailored to object dynamics in videos. Our experiments demonstrate that our method can effectively optimize a wide variety of rewards, with binary AI feedback driving the most significant improvements in video quality for dynamic interactions, as confirmed by both AI and human evaluations. Notably, we observe substantial gains when using reward signals derived from AI feedback, particularly in scenarios involving complex interactions between multiple objects and realistic depictions of objects falling.

1. Introduction

Large video generation models pre-trained on internet-scale videos have broad applications such as generating creative video content (Blattmann et al., 2023b; Ho et al., 2022a; Hong et al., 2022; Singer et al., 2022), creating novel games (Bruce et al., 2024), animations (Wang et al., 2019), movies (Zhu et al., 2023), and personalized educational content (Wang et al., 2024), as well as simulating the real-world (Brooks et al., 2024; Yang et al., 2023b) and controlling robots (Du et al., 2024; Ko et al., 2023). Despite these promises, state-of-the-art text-to-video models today still suffer from hallucination, generating unrealistic objects or movements that violate physics (Bansal et al., 2024; OpenAI, 2024; Yang et al., 2024), or even generating static scenes and ignoring specified movement altogether (Figure 1), which hinders the practical use of text-to-

video models.

Expanding both the dataset and the model size has proven effective in reducing undesirable behaviors in large language models (LLMs) (Hoffmann et al., 2022). However, when it comes to video generation, this scaling process is more complex. Creating detailed language labels for training text-to-video models is a labor-intensive task, and the architecture for video generation models has not yet reached a point where it can effectively scale in the same way language models have (Yang et al., 2024). In contrast, one of the most impactful advances in improving LLMs has been the integration of external feedback (Christiano et al., 2017; Ouyang et al., 2022). This raises important questions about what kinds of feedback can be gathered for text-to-video models and how these feedback can be integrated into the training of text-to-video models to re-



Figure 1 | Generated videos from open models: VideoCrafter (Chen et al., 2024) and VADER (Prabhudesai et al., 2024). Both pre-trained and RL-finetuned models fail to represent object movement in the prompts. Improving the dynamics of object interaction in the generated video is still an open problem.

duce hallucination and better align content with prompts.

In this paper, we investigate the recipe for improving dynamic interactions with objects in text-to-video diffusion models (Ho et al., 2022b) by leveraging external feedback. We cover various algorithms for self-improvement based on reinforcement learning (RL) and automated feedback for text-video alignment. We begin by noting that two representative offline optimization algorithms, reward-weighted regression (RWR) (Peters and Schaal, 2007) and direct preference optimization (DPO) (Rafailov et al., 2023), introduced independently in prior works, have stemmed from the same objective with some design choices such as KL-regularization and policy projection. Based on this observation, we derive a unified objective for RL-finetuning through the lens of probabilistic inference. For the choice of feedback, we test metric-based feedback on semantics (Radford et al., 2021), human preference (Kirstain et al., 2023; Wu et al., 2023a), and dynamics (Huang et al., 2024), and also propose leveraging the binary feedback obtained from large-scale vision-language models (VLMs) capable of video understanding.

Our experiments show that the proposed framework effectively maximizes various types of feedback, though iterative optimization poses challenges: RWR struggles with unseen prompts, while DPO over-optimizes metrics and suffers from visual collapse, making the best algorithm dependent on the desired generalization. Metric-based feedback, used in prior works (Li et al., 2024b; Prabhudesai et al., 2024; Yuan et al., 2023), poorly correlates with realistic object dynamics, as metric improvements don’t always

translate to plausible physics. In contrast, AI feedback from VLMs and human feedback better align with realistic dynamics, achieving the most significant improvements in scene quality. Lastly, we found that pre-trained video generation models struggle with multi-step interactions, new object appearances, and spatial 3D relationships, while RL fine-tuning helps address these limitations.

2. Preliminaries

Denosing Diffusion Probabilistic Models. We adopt denosing diffusion probabilistic models (DDPMs) (Ho et al., 2020; Sohl-Dickstein et al., 2015) for generating a H -frame video $\mathbf{x}_0 = [x_0^1, \dots, x_0^H]$. DDPM considers approximating the reverse process for data generation with a parameterized model $p_\theta(\mathbf{x}_0) = \int p_\theta(\mathbf{x}_{0:T}) d\mathbf{x}_{1:T}$, where $p_\theta(\mathbf{x}_{0:T}) = p(\mathbf{x}_T) \prod_{t=1}^T p_\theta(\mathbf{x}_{t-1} | \mathbf{x}_t)$, and $p(\mathbf{x}_T) = \mathcal{N}(0, I)$, $p_\theta(\mathbf{x}_{t-1} | \mathbf{x}_t) = \mathcal{N}(\mu_\theta(\mathbf{x}_t, t), \sigma_t^2 I)$. DDPM also has a forward process, where the Gaussian noise is iteratively added to the data with different noise level β_t : $q(\mathbf{x}_{1:T}) = \prod_{t=1}^T q(\mathbf{x}_t | \mathbf{x}_{t-1})$ and $q(\mathbf{x}_t | \mathbf{x}_{t-1}) = \mathcal{N}(\sqrt{1 - \beta_t} \mathbf{x}_{t-1}, \beta_t I)$. Considering the upper bound of negative log-likelihood $\mathbb{E}_q[-\log p_\theta(\mathbf{x}_0)]$ with practical approximations, we obtain the objective for DDPM $\mathcal{J}_{\text{DDPM}}$ as follows,

$$\mathbb{E}_q \left[\sum_{t=1}^T D_{\text{KL}}(q(\mathbf{x}_{t-1} | \mathbf{x}_t, \mathbf{x}_0) || p_\theta(\mathbf{x}_{t-1} | \mathbf{x}_t)) \right] \approx \mathbb{E}_{\mathbf{x}_0, \epsilon, t} \left[\|\epsilon - \epsilon_\theta(\sqrt{\alpha_t} \mathbf{x}_t + \sqrt{\beta_t} \epsilon, t)\|^2 \right] := \mathcal{J}_{\text{DDPM}}, \quad (1)$$

where $\alpha_t = 1 - \beta_t$. After training parameterized denosing model ϵ_θ , the video might be generated from the initial noise $\mathbf{x}_T \sim \mathcal{N}(\mathbf{0}, I)$

through the iterative denoising from $t = T$ to 1: $\mathbf{x}_{t-1} := \frac{1}{\sqrt{\alpha_t}} \left(\mathbf{x}_t - \frac{\beta_t}{\sqrt{\beta_t}} \epsilon_\theta(\mathbf{x}_t, t) \right) + \sigma_t u_t$, where $u_t \sim \mathcal{N}(0, I)$ and $\bar{\beta}_t = \prod_{s=1}^t \beta_s$. We also adopt text and first-frame conditioning $\mathbf{c} = [c_{\text{text}}, c_{x_0^1}]$ with classifier-free guidance (Ho and Salimans, 2022), and will consider the conditional formulation $p(\mathbf{x}_0 | \mathbf{c})$ in the following sections.

Probabilistic Inference View of RL-Finetuning Objectives. As in Fan et al. (2023) and Black et al. (2024), we formulate the denoising process in DDPMs as a T -horizon Markov decision process (MDP), which consists of the state $s_t = (\mathbf{x}_{T-t}, \mathbf{c})$, action $a_t = \mathbf{x}_{T-t-1}$, initial state distribution $P_0(s_0) = (\mathcal{N}(0, I), p(\mathbf{c}))$, transition function $P(s_{t+1} | s_t, a_t) = (\delta_{\{a_t\}}, \delta_{\{\mathbf{c}\}})$, reward function $R(s_t, a_t) = r(\mathbf{x}_0, \mathbf{c}) \mathbb{1}[t = T]$, and the policy $\pi_\theta(a_t | s_t) = p_\theta(\mathbf{x}_{T-t-1} | \mathbf{x}_{T-t}, \mathbf{c})$ where $\delta_{\{\cdot\}}$ is the Dirac distribution and $\mathbb{1}[\cdot]$ is a indicator function. Moreover, motivated by the probabilistic inference for control (Levine, 2018), we additionally introduce a binary event variable $O \in \{0, 1\}$ to this MDP, which represents if the generated video \mathbf{x}_0 is optimal or not. To derive the unified RL-finetuning objective for DDPM, we consider the log-likelihood $\log p(O = 1 | \mathbf{c})$ and decompose it with a variational distribution p' :

$$\begin{aligned} & \mathbb{E}_{p(\mathbf{c})} [\log p(O = 1 | \mathbf{c})] \\ &= \mathbb{E}_{p(\mathbf{c})p(\mathbf{x}_0|\mathbf{c})} \left[\log p(O = 1 | \mathbf{x}_0, \mathbf{c}) - \log \frac{p(\mathbf{x}_0 | \mathbf{c})}{p'(\mathbf{x}_0 | \mathbf{c})} \right] \\ & \quad + \mathbb{E}_{p(\mathbf{c})p(\mathbf{x}_0|\mathbf{c})} \left[\log \frac{p(\mathbf{x}_0 | \mathbf{c})}{p'(\mathbf{x}_0 | O = 1, \mathbf{c})} \right] \\ &= \mathcal{J}_{\text{RL}}(p, p') \\ & \quad + \mathbb{E}_{p(\mathbf{c})} [D_{\text{KL}}(p(\mathbf{x}_0 | \mathbf{c}) || p'(\mathbf{x}_0 | O = 1, \mathbf{c}))]. \end{aligned} \quad (2)$$

$\mathcal{J}_{\text{RL}}(p, p') := \mathbb{E} \left[\log p(O = 1 | \mathbf{x}_0, \mathbf{c}) - \log \frac{p(\mathbf{x}_0 | \mathbf{c})}{p'(\mathbf{x}_0 | \mathbf{c})} \right]$ is the evidence lower bound. As in the RL literature (Abdolmaleki et al., 2018; Furuta et al., 2021; Peters et al., 2010), we can assume the dependence on the reward such as $p(O = 1 | \mathbf{x}_0, \mathbf{c}) \propto \exp(\beta^{-1}r(\mathbf{x}_0, \mathbf{c}))$, because O stands for the optimality of the generated video. Then, we could rewrite $\mathcal{J}_{\text{RL}}(p, p')$ in an explicit

form of the unified objective for RL-finetuning:

$$\mathcal{J}_{\text{RL}}(p, p') := \mathbb{E} \left[\beta^{-1}r(\mathbf{x}_0, \mathbf{c}) - \log \frac{p(\mathbf{x}_0 | \mathbf{c})}{p'(\mathbf{x}_0 | \mathbf{c})} \right]. \quad (3)$$

In the following section, we will describe that existing algorithms can be derived from Equation 3 through the policy projection with expectation-maximization methods ($\mathcal{J}_{\text{f-EM}}$), or with Bradley-Terry assumptions (Bradley and Terry, 1952) ($\mathcal{J}_{\text{r-BT}}$), and characterize both types of objectives in the experiments.

3. RL-Finetuning with Feedback

We start with deriving the practical algorithms to optimize the unified objective for RL-finetuning (Section 3.1), provide a brief overview of metric-based feedback for the text-to-video models (Section 3.2), and then propose the pipeline for AI feedback from VLMs (Section 3.3).

3.1. Practical Algorithms

Equation 3 represents the general form of RL-finetuning objective for DDPM; which maximizes a reward under the KL-regularization (Levine, 2018). We derive the practical implementation; based on expectation-maximization, and on the Bradley-Terry assumptions. We cover and compare both algorithmic choices in the following experiments.

Forward-EM-Projection. This type of algorithm parameterizes $p' = p_\theta(\mathbf{x}_0 | \mathbf{c})$ and $p = p_{\text{ref}}(\mathbf{x}_0 | \mathbf{c})$ (i.e. forward KL-regularization), and perform coordinate ascent like a generic EM algorithm; solving Equation 3 with respect to the variational distribution p_{ref} while freezing the parametric posterior $p' = p_{\theta'}$ (E-step), and projecting the new $p_{\text{ref}}^{\text{new}}$ into the model parameter θ (M-Step). Specifically, E-step converts Equation 3 into the constraint optimization problem, and

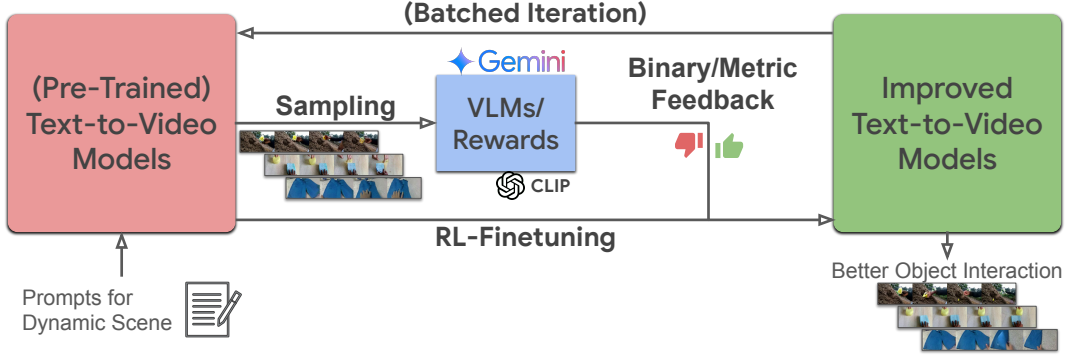


Figure 2 | A pipeline for RL-finetuning with feedback. We first generate videos from the pre-trained models, and then use VLMs capable of video understanding (or metric-based reward) to obtain feedback labels. Those data are leveraged for offline and iterative RL-finetuning.

considers the following Lagrangian:

$$\begin{aligned}
 & \mathcal{J}_{\text{RL}}(p_{\text{ref}}, \lambda) \\
 &= \int p(\mathbf{c}) \int p_{\text{ref}}(\mathbf{x}_0 | \mathbf{c}) \beta^{-1} r(\mathbf{x}_0, \mathbf{c}) d\mathbf{x}_0 d\mathbf{c} \\
 & - \int p(\mathbf{c}) \int p_{\text{ref}}(\mathbf{x}_0 | \mathbf{c}) \log \frac{p_{\text{ref}}(\mathbf{x}_0 | \mathbf{c})}{p_{\theta'}(\mathbf{x}_0 | \mathbf{c})} d\mathbf{x}_0 d\mathbf{c} \\
 & + \lambda \left(1 - \int p(\mathbf{c}) \int p_{\text{ref}}(\mathbf{x}_0 | \mathbf{c}) d\mathbf{x}_0 d\mathbf{c} \right).
 \end{aligned} \tag{4}$$

The analytical solution of Equation 4 is $p_{\text{ref}}^{\text{new}}(\mathbf{x}_0 | \mathbf{c}) = \frac{1}{Z(\mathbf{c})} p_{\theta'}(\mathbf{x}_0 | \mathbf{c}) \exp(\beta^{-1} r(\mathbf{x}_0, \mathbf{c}))$, where $Z(\mathbf{c})$ is the partition function. M-step projects the non-parametric optimal model $p_{\text{ref}}^{\text{new}}$ to the parametric model by maximizing Equation 3 with respect to p_{θ} :

$$\begin{aligned}
 & \mathcal{J}_{\text{RL}}(\theta) \\
 &= -\mathbb{E}_{p(\mathbf{c})p_{\text{ref}}^{\text{new}}} [\log p_{\theta}(\mathbf{x}_0 | \mathbf{c})] \\
 &= -\mathbb{E}_{p(\mathbf{c})p_{\theta'}} \left[\frac{1}{Z(\mathbf{c})} \exp(\beta^{-1} r(\mathbf{x}_0, \mathbf{c})) \log p_{\theta}(\mathbf{x}_0 | \mathbf{c}) \right].
 \end{aligned} \tag{5}$$

To stabilize the training, RWR (Lee et al., 2023b; Peters and Schaal, 2007) for diffusion models simplifies $\mathcal{J}_{\text{RL}}(\theta)$ by removing the intractable normalization $Z(\mathbf{c})$, setting pre-trained models p_{pre} into $p_{\theta'}$, converting exponential transform into the identity mapping, and considering the simplified upper-bound of negative log-likelihood which

results in the practical minimization objective:

$$\begin{aligned}
 & -\mathbb{E}_{p(\mathbf{c})p_{\theta'}} [r(\mathbf{x}_0, \mathbf{c}) \log p_{\theta}(\mathbf{x}_0 | \mathbf{c})] \\
 & \approx \mathbb{E}_{\mathbf{c}, \mathbf{x}_0, \epsilon, t} \left[r(\mathbf{x}_0, \mathbf{c}) \|\epsilon - \epsilon_{\theta}(\sqrt{\alpha_t} \mathbf{x}_t + \sqrt{\beta_t} \epsilon, \mathbf{c}, t)\|^2 \right] \\
 & := \mathcal{J}_{\text{f-EM}}.
 \end{aligned} \tag{6}$$

Reverse-BT-Projection. This category parameterizes $p = p_{\theta}(\mathbf{x}_0 | \mathbf{c})$ and $p' = p_{\text{ref}}(\mathbf{x}_0 | \mathbf{c})$ (i.e. reverse KL-regularization). For instance, PPO (Black et al., 2024; Fan et al., 2023; Schulman et al., 2017) optimizes Equation 3 with a policy gradient. However, such on-policy policy gradient methods require massive computational costs and would be unstable for the text-to-video models. Alternatively, we consider the lightweight approach by optimizing the surrogate objective to extract the non-parametric optimal model into the parametric data distribution p_{θ} as in DPO (Rafailov et al., 2023; Wallace et al., 2023). First, we introduce the additional Bradley-Terry assumption (Bradley and Terry, 1952), where, if one video $\mathbf{x}_0^{(1)}$ is more preferable than another $\mathbf{x}_0^{(2)}$ (i.e. $\mathbf{x}_0^{(1)} > \mathbf{x}_0^{(2)}$), the preference probability $p(\mathbf{x}_0^{(1)} > \mathbf{x}_0^{(2)} | \mathbf{c})$ is a function of reward $r(\mathbf{x}_0, \mathbf{c})$ such as,

$$p(\mathbf{x}_0^{(1)} > \mathbf{x}_0^{(2)} | \mathbf{c}) = \sigma(r(\mathbf{x}_0^{(1)}, \mathbf{c}) - r(\mathbf{x}_0^{(2)}, \mathbf{c})), \tag{7}$$

where $\sigma(\cdot)$ is a sigmoid function. Transforming analytical solution of Equation 4 into $p_{\theta}(\mathbf{x}_0 | \mathbf{c}) = \frac{1}{Z(\mathbf{c})} p_{\text{ref}}(\mathbf{x}_0 | \mathbf{c}) \exp(\beta^{-1} r(\mathbf{x}_0, \mathbf{c}))$, we can obtain the parameterized reward $r_{\theta}(\mathbf{x}_0, \mathbf{c}) =$



Figure 3 | Example videos from Something-Anything-V2. We define five principles of challenging object movements: object removal (OR), multiple objects (MO), deformable object (DO), directional movement (DM), and falling down (FD).

$\beta \log \frac{p_\theta(\mathbf{x}_0|\mathbf{c})}{p_{\text{ref}}(\mathbf{x}_0|\mathbf{c})} + \beta \log Z(\mathbf{c})$. The surrogate objective is maximizing the log-likelihood of preference probability by substituting r_θ into Equation 7 and considering the simplified lower-bound of log-likelihood:

$$\begin{aligned}
 & -\mathbb{E}_{\mathbf{x}_0^{(1:2)}, \mathbf{c}} \left[\log p(\mathbf{x}_0^{(1)} > \mathbf{x}_0^{(2)} | \mathbf{c}) \right] \\
 & = -\mathbb{E}_{\mathbf{x}_0^{(1:2)}, \mathbf{c}} \left[\log \sigma \left(\beta \log \frac{p_\theta(\mathbf{x}_0^{(1)} | \mathbf{c}) p_{\text{ref}}(\mathbf{x}_0^{(2)} | \mathbf{c})}{p_{\text{ref}}(\mathbf{x}_0^{(1)} | \mathbf{c}) p_\theta(\mathbf{x}_0^{(2)} | \mathbf{c})} \right) \right] \\
 & \approx -\mathbb{E}_{\mathbf{x}_0^{(1:2)}, \mathbf{c}, \epsilon, t} \left[\log \sigma \left(\beta (\|\epsilon - \epsilon_\theta^{(1)}\|^2 - \|\epsilon - \epsilon_{\text{ref}}^{(1)}\|^2 \right. \right. \\
 & \quad \left. \left. - \|\epsilon - \epsilon_\theta^{(2)}\|^2 + \|\epsilon - \epsilon_{\text{ref}}^{(2)}\|^2) \right) \right] \\
 & := \mathcal{J}_{\text{r-BT}},
 \end{aligned} \tag{8}$$

where we shorten $\epsilon_\theta(\sqrt{\alpha_t}\mathbf{x}_t^{(1)} + \sqrt{\beta_t}\epsilon, \mathbf{c}, t)$ as $\epsilon_\theta^{(1)}$.

3.2. Metric-based Reward for RL-finetuning

With the algorithms introduced in Section 3.1, we may choose any reward to be optimized. Prior works on finetuning text-to-image models (Black et al., 2024; Fan et al., 2023) have often employed metric-based feedback as a reward to improve the visual quality, style of images, and text-image alignment. The metric-based rewards are popular because they can amortize the costs to collect actual human feedback (Lee et al., 2023b), and

can propagate the gradient through the parameterized evaluators (Clark et al., 2024). Even for text-to-video models (Li et al., 2024b; Prabhudesai et al., 2024; Yuan et al., 2023), such frame-wise metrics have been primary choices. Following prior works, we examine several metric-based feedback:

CLIP score (Radford et al., 2021). Leveraging CLIP is one of the most popular methods to evaluate the generative models in terms of text-image alignment, which can reflect the semantics of the scene to a single metric. We use ViT-B16 (Dosovitskiy et al., 2020) for the backbone model and sum the scores over the frames.

HPSv2 (Wu et al., 2023a,b) and PickScore (Kirstain et al., 2023). These models could predict the human preference for the generated images, because they are trained on large-scale preference data, curated from DiffusionDB (Wang et al., 2022), COCO Captions (Chen et al., 2015), and various text-to-image models. They use OpenCLIP (Ilharco et al., 2021) with ViT-H14 and take both image and text as inputs. We also sum these scores over the frames.

Methods	CLIP		HPSv2		PickScore		Optical Flow		AI Feedback	
	Train	Test	Train	Test	Train	Test	Train	Test	Train	Test
Pre-Trained	1.9240	1.9275	1.8139	1.7772	1.5697	1.5637	370.2	409.6	53.02%	51.56%
SFT	1.9287	1.9270	1.8114	1.7748	1.5698	1.5639	368.6	416.4	55.94%	47.50%
RWR (\mathcal{J}_{f-EM})	1.9309	1.9289	1.8132	1.7776	1.5699	1.5644	375.0	422.0	58.23%	50.94%
DPO (\mathcal{J}_{f-BT})	1.9259	1.9325	1.8160	1.7797	1.5701	1.5641	377.8	410.7	56.56%	55.00%

Table 1 | Performance of text-to-video models after RL-finetuning, optimizing each reward by each algorithm independently. The color indicates the metric is **improved** or **worsen** compared to pre-trained models. RL-finetuning (RWR and DPO) can improve most metrics compared to pre-trained models or SFT (baseline without reward signal), and exhibits better generalization to unseen test prompts. In these cases, DPO increases all the metrics and often achieves better performance than RWR.

Optical Flow (Huang et al., 2024). While assessing the semantics per frame, we should also consider the dynamic degree in the generations. The dynamic object movement can be captured with the optical flow between the successive two frames. Following prior works (Huang et al., 2024; Ju et al., 2024), we use RAFT (Teed and Deng, 2020) to estimate the optical flow, take the average of norm among the top-5% as a single metric, and sum them over the frames.

In practice, we adopt reward shaping via linear transformation for each metric-based reward to control the scale of gradients (Fan et al., 2023): $r_{lin}(\mathbf{x}_0, \mathbf{c}) = \eta r(\mathbf{x}_0, \mathbf{c}) + \gamma$ where $\eta > 0$ is a scaling and $\gamma \geq 0$ is a shifting factor. The scaling factor is important to the optical flow, and the shifting factor to other metrics (CLIP, HPSv2, and PickScore). We test a range of constant factors, such as $\eta \in \{0.005, 0.0075, 0.01, 0.1, 1.0\}$ and $\gamma \in \{0, 0.5, 0.75, 1.0\}$, and report the best results.

3.3. AI Feedback from Vision-Language Models

One of the most reliable evaluations of any generative model can be feedback from humans, while human evaluation requires a lot of costs. One scalable way to replace subjective human evaluation is AI feedback (Bai et al., 2022; Wu et al., 2024c), which has succeeded in improving LLMs (Lee et al., 2023a). Inspired by this, we propose employing VLMs, capable of video understanding, to obtain the AI feedback for text-to-video models.

We provide the textual prompt and video as inputs and ask VLMs to evaluate the input video in terms of overall coherence, physical accuracy,

task completion, and the existence of inconsistencies. The feedback VLMs predict is a binary label; accepting the video if it is coherent and the task is completed, or rejecting it if it does not satisfy any evaluation criteria. We find that reasoning or explaining the rationale does not help to improve the accuracy. For VLMs, we use Gemini-1.5-Pro (Gemini Team, 2023). See Appendix B for the prompts to elicit feedback on the text-content alignment.

Pair-Wise and Point-Wise Feedback. When using a VLM to provide feedback for the generated videos, we have the option of comparing two generations at once or scoring each generation individually, similar to the reward used to train language models with human feedback (Qin et al., 2023). As a preliminary, we experiment with both types of feedback with the a priori that the true video is always preferable. We found that for pair-wise feedback, the true videos are preferable to generated videos for only 62.5% of the time. Meanwhile, for point-wise feedback, the true videos are preferable to generated videos for 90.3% of the time. As a result, we focus on using binary point-wise feedback in this work.

4. Experiments

We first describe the experimental setup and the dataset composition for realistic video generation with dynamic object movement (Section 4.1). In the experiments, we examine whether RL-finetuning can increase each metric compared to SFT on self-generated data (Section 4.2), and investigate which combination of algorithms and

Method+Reward	AI Eval			Human Eval		
	Train	Test	All	Train	Test	All
Pre-Trained	53.02%	51.56%	52.66%	19.79%	18.13%	19.38%
SFT	55.94%	47.50%	53.83%	23.65%	13.44%	21.09%
RWR-CLIP	55.31%	45.00%	52.73%	27.19%	12.50%	23.52%
RWR-HPSv2	52.92%	57.50%	54.06%	26.04%	21.56%	24.92%
RWR-PS	55.52%	49.69%	54.06%	25.73%	11.56%	22.19%
RWR-OptFlow	57.81%	50.00%	55.86%	28.75%	10.00%	24.06%
RWR-AIF	58.23%	50.94%	56.41%	33.65%	23.44%	31.09%
DPO-CLIP	52.29%	54.38%	52.81%	24.90%	23.44%	24.53%
DPO-HPSv2	55.73%	51.56%	54.69%	26.35%	25.00%	26.02%
DPO-PS	53.02%	55.31%	53.59%	25.94%	22.50%	25.08%
DPO-OptFlow	54.06%	54.06%	54.06%	26.88%	24.06%	26.17%
DPO-AIF	56.56%	55.00%	56.17%	36.04%	28.13%	34.06%

Table 2 | VLM and human preference evaluation among the combination of algorithms and rewards. {algorithm}–{reward} stands for finetuning text-to-video models by optimizing {reward} with {algorithm}. AI feedback from VLMs (RWR-AIF and DPO-AIF) achieves the best alignment, compared to any metric-based rewards. RWR may achieve better alignment on the train split than DPO while exhibiting *over-fitting*, where the performance on the test split degrades from pre-trained models.

rewards can improve the text-content alignment the most through AI and human evaluation (Section 4.3). Moreover, we analyze the relationship between human preference and other types of automated feedback (Section 4.4).

Experimental Setup. We pre-train video diffusion models based on 3D-UNet (Özgün Çiçek et al., 2016) with Something-Something-V2 dataset until converged, which obtains a good prior model for realistic object movements. As explained in Section 4.1, we prepare 5×24 prompts for training and 5×8 prompts for evaluation and generate 128 samples per each prompt in the train split from pre-trained models to collect the data for finetuning. We then put the AI feedback and reward labels on the generated videos. For the evaluation, we generate 32 videos per prompt, compute each metric per video summing them over the frames, and average over top-8 samples. Under the same instruction as VLMs for the binary AI evaluation, we also conduct a human evaluation with binary rating. The whole pipeline is summarized in Figure 2.

4.1. A Set of Challenging Object Movements

While state-of-the-art text-to-video models can generate seemingly realistic videos, the gener-

ated sample often contains static scenes ignoring the specified behaviors, movement violating the physical laws and appearing out-of-place objects (Figure 1), which can be attributed as an insufficient text-content alignment in video generation (Bansal et al., 2024; Liu et al., 2024). To characterize the hallucinated behavior of text-to-video models in a dynamic scene, we curate dynamic and challenging object movements from a pair of prompt and reference videos. From an empirical observations, we define the following five categories as challenging object movements:

- **Object Removal:** To move something out from the container in the scene, or the camera frame itself. A transition to a new scene often induces out-of-place objects. For example, *taking a pen out of the box*.
- **Multiple Objects:** Object interaction with multiple instances. In a dynamic scene, it is challenging to keep the consistency of all the contents. For example, *moving lego away from mouse*.
- **Deformable Object:** To manipulate deformable objects, such as cloths and paper. The realistic movement of non-rigid instances requires sufficient expressibility and can test the text-content alignment. For example, *twisting shirt wet until water comes out*.
- **Directional Movement:** To move something in a specified direction. Text-to-video models can roughly follow the directions in the prompts, although they often fail to generate consistent objects in the scene. For example, *pulling water bottle from left to right*.
- **Falling Down:** To fall something down. This category often requires the dynamic expression towards the depth dimension. For example, *putting marker pen onto plastic bottle so it falls off the table*.

As a realistic object movement database, we use Something-Something-V2 dataset (Goyal et al., 2017; Mahdisoltani et al., 2018). We carefully select 32 prompts and videos per category from the validation split, using 24 prompts for train data and 8 for test data (Figure 3). See Appendix A for the list of prompts. Moreover, the quantitative evaluation of whether the generated samples can simulate realistic physical laws is one of the major challenges. In this paper, we employ human

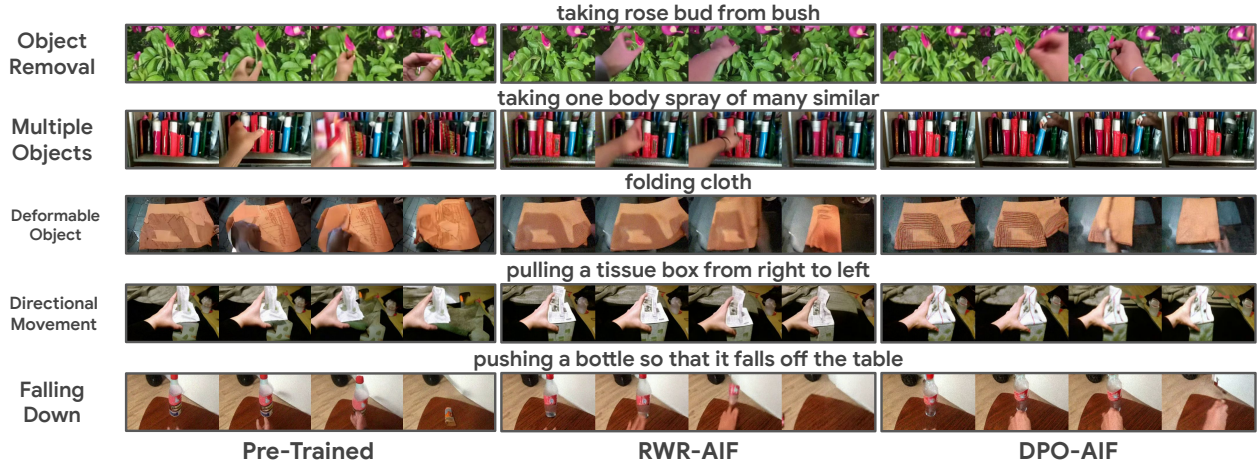


Figure 4 | Generated videos from pre-trained models, RWR-AIF, and DPO-AIF. RL-finetuning enhances the alignment where the video follows the prompt. See Appendix F for other examples. We also provide the detailed takeaways for algorithm designs in Appendix E.

and AI evaluation (from VLMs) to measure the acceptance rate.

4.2. RL-Finetuning Works for Any Quality Metric

Table 1 presents the alignment performance, measured by each reward, in text-to-video generation after finetuning. We finetune and evaluate the models for each combination of feedback and algorithm independently. RWR and DPO, RL-finetuning with feedback, can improve most metrics, including AI feedback, compared to pre-trained models, and supervised finetuning (SFT) baseline that does not leverage any reward signal. In addition, RWR and DPO exhibit better generalization to hold-out prompts than SFT. These can justify the usage of RL-finetuning with feedback to improve the text-content alignment for the dynamic scene. Comparing RWR and DPO, DPO increases all the evaluation metrics and often achieves better performance than RWR (7 in 10 metrics), which implies that subtle algorithmic choices, such as a direction of KL-regularization, on the unified objective would be a significant difference for RL-finetuning.

4.3. VLMs as the Best Proxy for Human Preference

We here aim to identify what kind of algorithms and metrics can improve the text-content align-

ment of dynamic object movement in text-to-video models. Table 2 provides the preference evaluation among all the combinations of algorithms and rewards, which are assessed through binary feedback by VLMs and humans. The results reveal that, while all the rewards could realize the improvement, RL-finetuning with AI feedback from VLMs (RWR-AIF and DPO-AIF) achieve the best alignment performance, compared to any metric-based single rewards; RWR-AIF achieves +3.8% in AI evaluation (52.66% \rightarrow 56.41%), and +11.8% in human evaluation (19.38% \rightarrow 31.09%). DPO-AIF achieves +3.5% (52.66% \rightarrow 56.17%), and +14.7% (19.38% \rightarrow 34.06%) as an absolute gain. VLMs can work as the best proxy of human evaluators to realize efficient text-content alignment (Figure 4).

Comparing RWR and DPO, RWR tends to achieve better alignment on the train split, while also exhibiting the *over-fitting* behaviors, where the performance against the test splits degrades from the pre-trained models. On the other hand, DPO does not face over-fitting and robustly aligns the output to be preferable, ensuring the generalization. Because SFT faces over-fitting issues too, we guess the lack of negative gradients that push down the likelihood of bad samples might cause insufficient generalization (Tajwar et al., 2024).

Iterative RL-Finetuning on AI Feedback. Our proposal (Figure 2) can extend to iterative fine-



Figure 5 | **(Left)** Over-optimization issues in metric-based feedback. While DPO-HPSv2 could improve HPSv2 as the gradient step increases, the ratio of video accepted by VLMs significantly decreases. **(Right)** Generated videos from the models over-optimized with DPO-HPSv2. The model just makes the tone of the frames dark, without any improvement on the dynamics.

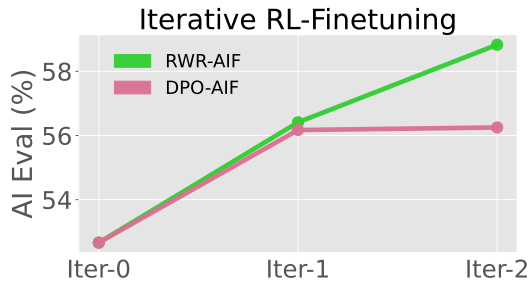


Figure 6 | Preference evaluation after iterative RL-finetuning with AI feedback. RWR-AIF continually improves its outputs by leveraging on-policy samples, while DPO-AIF seems to be saturated.

tuning, which can resolve distribution shift issues in offline finetuning (Matsushima et al., 2021; Xu et al., 2023a) and leads to further alignment to preferable outputs. Figure 6 shows that RWR-AIF continually improves its output by leveraging self-generations (52.66% \rightarrow 56.41% \rightarrow 58.83%), while DPO-AIF is saturated (52.66% \rightarrow 56.17% \rightarrow 56.25%). This can be because the paired data from one-iteration DPO becomes equally good due to the overall improvement; it is hard to assign binary preferences correctly.

Over-Optimization in DPO with Metrics-based Reward. We also find that finetuning metrics-based rewards with DPO, such as HPSv2 or PickScore, faces over-optimization issues (Azar et al., 2023; Furuta et al., 2024), where the metrics are improving while the generated videos are visually worsened to the humans. For instance, in Figure 5, while DPO-HPSv2 could improve HPSv2 as the gradient step increases, the ratio of acceptable video through the AI evalua-

tion, significantly decreases, which implies that metric-based rewards, even if trained on human preferences, may not always be good proxies for perceived human evaluation. It is probably important for scalable text-to-video improvement to incorporate the supervision process by the capable VLMs, not limited to leveraging automated external feedback just for finetuning.

4.4. Correlation with Human Evaluation

We also analyze the correlation between human preference and automated feedback, such as AI feedback from VLMs, and metric-based rewards (CLIP, HPSv2, PickScore, and Optical Flow). As done in Table 2 for AI/human evaluation, we first measure the average of each metric per algorithm-feedback combination (such as SFT, RWR-CLIP, DPO-AIF, etc), and compute Pearson correlation coefficient to the human preference (Figure 7; left). The results reveal that the performance measured with AI preference from VLMs has the most significant positive correlation to the one with human preference ($R = 0.746$; statistically significant with $p \leq 0.01$), while others only exhibit weak correlations, which supports the observation that optimizing AI feedback can be the best proxy for optimizing the human feedback.

In contrast, when we measure the correlation between the averaged human preference and automated feedback among the $32 \times 5 = 160$ prompts (Figure 7; right), human preference exhibits weak positive correlation only to AI preference ($R = 0.231$; statistically significant with $p \leq 0.01$), and others does not have notable correlations. This implies that even with the best

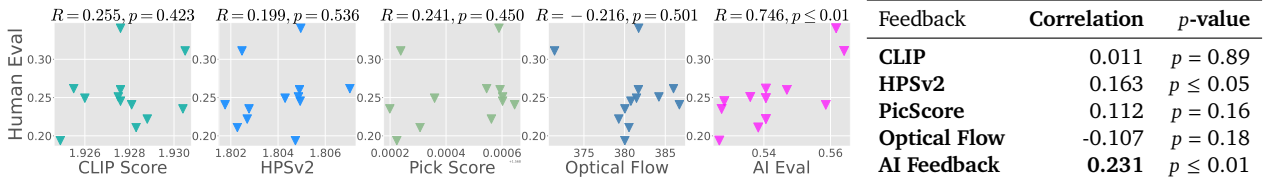


Figure 7 | **(Left)** Pearson correlation coefficient between the performance with human preference and with other automated feedback, among 12 algorithm-reward combinations. AI preference from VLMs has the best positive correlation to human preference ($R = 0.746$; statistically significant with $p \leq 0.01$). **(Right)** Correlation between the averaged human preference and the averaged automated feedback, among $32 \times 5 = 160$ prompts. Even the best AI feedback only exhibits a weak positive correlation ($R = 0.231$ with $p \leq 0.01$). The rationale of preference from VLMs is still not enough to be aligned with humans, despite the promising quality improvement.

choice – AI feedback from VLMs, the rationale of preference is still not enough to be perfectly aligned with human feedback (Wu et al., 2024b). While we demonstrate the promising signal to leverage VLMs to improve the quality of dynamic object interaction in text-to-video models, we also call for the improvement of VLMs to be calibrated with human perception.

5. Discussion and Limitation

Analysis on Generated Object Movement. We analyze the trend of generated video before/after RL-finetuning among five categories of challenging object movement. Figure 8 (left) shows the AI preference (above) and absolute improvement (below) from pre-trained models per category. Generally, text-to-video models generate preferable videos of deformable objects (DO) and directional movement (DM) which are often complete with two-dimensional movement from the first frame. In contrast, they may not be good at modeling multi-step interactions, the appearance of new objects, and spatial three-dimensional relationships, which often occur in object removal (OR), multiple objects (MO), and falling down (FD). For instance, Figure 8 (right) requires multi-step interactions, such as opening a drawer, picking up a bottle opener, and putting it in the drawer, but the generated video is stuck in the first step (see Appendix G for other failures). RL-finetuning notably improves video generation in the category of multiple objects and falling down, probably because it is relatively easy for VLMs to judge if such a generation is acceptable or not.

Future Directions. While the scalable qualitative evaluation of video generation has been a long-standing problem (Dai et al., 2024; He et al., 2024; Liao et al., 2024; Liu et al., 2023; Miao et al., 2024; Wu et al., 2024a), we demonstrate that VLMs can be an automated solution, and AI feedback can provide informative signals to improve the dynamic scene generation. However, currently, there are only a few VLMs sufficiently capable of video understanding, such as Gemini (Gemini Team, 2023). It is also necessary to improve VLMs for quality judgments.

Due to the cost of querying VLMs online for AI feedback, the lack of a standard recipe to train a text-video reward, and the hyperparameter sensitivity of policy gradient methods, this paper focuses on offline and iterative RL-finetuning. Considering the performance gain coming from online samples, it is a natural yet important direction to resolve the bottlenecks above and extend ours to naive online RL methods (Black et al., 2024; Fan et al., 2023). Moreover, prior works have actively leveraged direct reward gradient from the differentiable metric-based rewards to align text-to-image (Clark et al., 2024; Prabhudesai et al., 2023), or even text-to-video models (Prabhudesai et al., 2024). In contrast, a recent study in LLMs (Zhang et al., 2024a) has argued that generative reward modeling can benefit from several advantages of LLMs and achieves better performance. The comprehensive analysis of AI feedback from the generative VLMs, compared to differentiable rewards is another important topic.

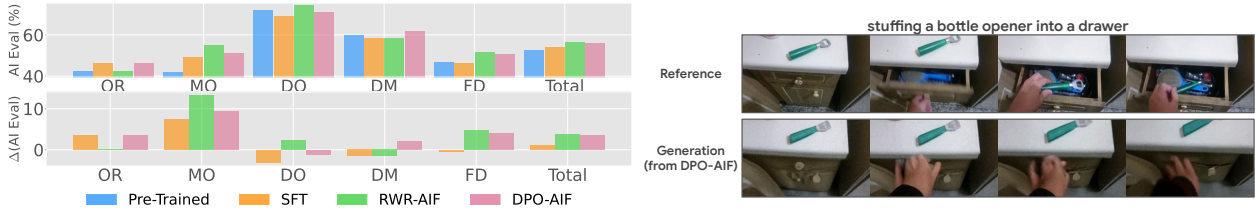


Figure 8 | (Left) Analysis of preferable generation per category with AI evaluation (above) and absolute improvement from pre-trained models (below). Text-to-video models generate high-quality videos of deformable object and directional movement, while not good at generating scenes of object removal, multiple objects, and falling down. AI feedback notably increases preferable outputs in multiple objects and falling down. (Right) Failure generation, which cannot express multi-step interaction. See Appendix G for other examples.

6. Related Works

RL for Text-to-Image Generation. Inspired by RL with human feedback for LLMs (Ouyang et al., 2022), there has been a great interest in employing RL-finetuning to better align text-to-image diffusion models (Kim et al., 2024; Lee et al., 2023b). RL-finetuning for diffusion models has a lot of variants such as policy gradient (Black et al., 2024; Fan et al., 2023; Uehara et al., 2024; Zhang et al., 2024b,c) based on PPO (Schulman et al., 2017), offline methods (Dong et al., 2023; Lee et al., 2023b; Liang et al., 2024; Na et al., 2024; Wallace et al., 2023; Yang et al., 2023a; Yuan et al., 2024) based on DPO (Rafailov et al., 2023) or RWR (Peng et al., 2019; Peters and Schaal, 2007), and direct reward gradients (Clark et al., 2024; Prabhudesai et al., 2023). These work often optimize compressibility (Black et al., 2024), aesthetic quality (Ke et al., 2023), or human preference (Li et al., 2024a; Xu et al., 2023b), and show that RL-finetuning effectively aligns pre-trained diffusion models to specific downstream objectives. Our work focuses on aligning text-to-video models, which can be more challenging as videos have much complex temporal information, and it is unclear whether feedback developed for aligning text-to-image models can be directly applied to text-to-video.

RL for Text-to-Video Generation. There has also been a few recent work that explored fine-tuning text-to-video models with reward feedback (Li et al., 2024b; Prabhudesai et al., 2024; Yuan et al., 2023). These work leverage open text-to-video models (Blattmann et al., 2023a;

Chen et al., 2024; Wang et al., 2023; Zheng et al., 2024b), and off-the-shelf text-to-image reward models, whose gradients are used to align the models to aesthetic or visual quality objective rather than the dynamics in the scenes. However, because there is no standard protocol to collect comprehensive feedback for reward modeling, the reward to directly evaluate generated video has been rarely considered. Furthermore, policy-gradient-based methods are sensitive to hyper-parameters and not stable (Rafailov et al., 2023). Our work differs from existing work in exploring a wide array of feedback to see if they can optimize the object movement rather than visual style, leveraging offline learning to bypass the need for learning a reward model, as well as considering AI feedback from VLMs as a proxy for human preference to generated videos, which has great potential as VLMs continue to improve.

In Appendix D, we further discuss additional related works on AI feedback for LLMs.

7. Conclusion

We thoroughly examine design choices to improve the dynamic scenes in text-to-video generation. Our proposal, combining (iterative) RL-finetuning with AI feedback from VLMs, could improve the text-video alignment best, rather than other metric-based rewards. RL-finetuning may mitigate the issues in modeling multi-step interactions, the appearance of new objects, and spatial relationships. Despite the promise, we also point out the necessity of VLMs to be further calibrated with humans. We hope this work helps text-video alignment in object movement further.

Acknowledgements

We thank Izzeddin Gur, Yusuke Iwasawa and Doina Precup for helpful discussion and reviewing initial version of this work. HF was supported by JSPS KAKENHI Grant Number JP22J21582.

References

- A. Abdolmaleki, J. T. Springenberg, Y. Tassa, R. Munos, N. Heess, and M. Riedmiller. Maximum a posteriori policy optimisation. In *International Conference on Learning Representations*, 2018.
- R. Agarwal, A. Singh, L. M. Zhang, B. Bohnet, S. Chan, A. Anand, Z. Abbas, A. Nova, J. D. Co-Reyes, E. Chu, et al. Many-shot in-context learning. *arXiv preprint arXiv:2404.11018*, 2024.
- M. G. Azar, M. Rowland, B. Piot, D. Guo, D. Calandriello, M. Valko, and R. Munos. A general theoretical paradigm to understand learning from human preferences. *arXiv preprint arxiv:2310.12036*, 2023.
- Y. Bai, S. Kadavath, S. Kundu, A. Askell, J. Kernion, A. Jones, A. Chen, A. Goldie, A. Mirhoseini, C. McKinnon, C. Chen, C. Olsson, C. Olah, D. Hernandez, D. Drain, D. Ganguli, D. Li, E. Tran-Johnson, E. Perez, J. Kerr, J. Mueller, J. Ladish, J. Landau, K. Ndousse, K. Lukosuite, L. Lovitt, M. Sellitto, N. Elhage, N. Schiefer, N. Mercado, N. DasSarma, R. Lasenby, R. Larson, S. Ringer, S. Johnston, S. Kravec, S. E. Showk, S. Fort, T. Lanham, T. Telleen-Lawton, T. Conerly, T. Henighan, T. Hume, S. R. Bowman, Z. Hatfield-Dodds, B. Mann, D. Amodei, N. Joseph, S. McCandlish, T. Brown, and J. Kaplan. Constitutional ai: Harmlessness from ai feedback. *arXiv preprint arXiv:2212.08073*, 2022.
- H. Bansal, Z. Lin, T. Xie, Z. Zong, M. Yarom, Y. Bitton, C. Jiang, Y. Sun, K.-W. Chang, and A. Grover. Video-phy: Evaluating physical commonsense for video generation. *arXiv preprint arXiv:2406.03520*, 2024.
- K. Black, M. Janner, Y. Du, I. Kostrikov, and S. Levine. Training diffusion models with reinforcement learning. In *The Twelfth International Conference on Learning Representations*, 2024.
- A. Blattmann, T. Dockhorn, S. Kulal, D. Mendelevitch, M. Kilian, D. Lorenz, Y. Levi, Z. English, V. Voleti, A. Letts, V. Jampani, and R. Rombach. Stable video diffusion: Scaling latent video diffusion models to large datasets. *arXiv preprint arXiv:2311.15127*, 2023a.
- A. Blattmann, R. Rombach, H. Ling, T. Dockhorn, S. W. Kim, S. Fidler, and K. Kreis. Align your latents: High-resolution video synthesis with latent diffusion models. In *IEEE Conference on Computer Vision and Pattern Recognition (CVPR)*, 2023b.
- R. A. Bradley and M. E. Terry. Rank analysis of incomplete block designs: I. the method of paired comparisons. *Biometrika*, 39(3/4):324–345, 1952.
- T. Brooks, B. Peebles, C. Holmes, W. DePue, Y. Guo, L. Jing, D. Schnurr, J. Taylor, T. Luhman, E. Luhman, C. Ng, R. Wang, and A. Ramesh. Video generation models as world simulators, 2024. URL <https://openai.com/research/video-generation-models-as-world-simulators>.
- J. Bruce, M. Dennis, A. Edwards, J. Parker-Holder, Y. Shi, E. Hughes, M. Lai, A. Mavalankar, R. Steigerwald, C. Apps, et al. Genie: Generative interactive environments. *arXiv preprint arXiv:2402.15391*, 2024.
- H. Chen, Y. Zhang, X. Cun, M. Xia, X. Wang, C. Weng, and Y. Shan. Videocrafter2: Overcoming data limitations for high-quality video diffusion models. *arXiv preprint arXiv:2401.09047*, 2024.
- X. Chen, H. Fang, T.-Y. Lin, R. Vedantam, S. Gupta, P. Dollar, and C. L. Zitnick. Microsoft coco captions: Data collection and evaluation server. *arXiv preprint arXiv:1504.00325*, 2015.
- P. Christiano, J. Leike, T. B. Brown, M. Martic, S. Legg, and D. Amodei. Deep reinforcement learning from human preferences. *arXiv preprint arXiv:1706.03741*, 2017.
- K. Clark, P. Vicol, K. Swersky, and D. J. Fleet. Directly fine-tuning diffusion models on differentiable rewards. In *The Twelfth International Conference on Learning Representations*, 2024.
- J. Dai, T. Chen, X. Wang, Z. Yang, T. Chen, J. Ji, and Y. Yang. Safesora: Towards safety alignment of text2video generation via a human preference dataset. *arXiv preprint arXiv:2406.14477*, 2024.
- H. Dong, W. Xiong, D. Goyal, Y. Zhang, W. Chow, R. Pan, S. Diao, J. Zhang, K. SHUM, and T. Zhang. RAFT: Reward ranked finetuning for generative foundation model alignment. *Transactions on Machine Learning Research*, 2023. ISSN 2835-8856.
- A. Dosovitskiy, L. Beyer, A. Kolesnikov, D. Weissenborn, X. Zhai, T. Unterthiner, M. Dehghani, M. Minderer, G. Heigold, S. Gelly, et al. An image is worth 16x16 words: Transformers for image recognition at scale. *arXiv preprint arXiv:2010.11929*, 2020.

- Y. Du, S. Yang, B. Dai, H. Dai, O. Nachum, J. Tenenbaum, D. Schuurmans, and P. Abbeel. Learning universal policies via text-guided video generation. *Advances in Neural Information Processing Systems*, 36, 2024.
- Y. Fan, O. Watkins, Y. Du, H. Liu, M. Ryu, C. Boutilier, P. Abbeel, M. Ghavamzadeh, K. Lee, and K. Lee. Reinforcement learning for fine-tuning text-to-image diffusion models. In *Thirty-seventh Conference on Neural Information Processing Systems*, 2023.
- H. Furuta, T. Kozuno, T. Matsushima, Y. Matsuo, and S. S. Gu. Co-adaptation of algorithmic and implementational innovations in inference-based deep reinforcement learning. In *Advances in Neural Information Processing Systems*, 2021.
- H. Furuta, K.-H. Lee, S. S. Gu, Y. Matsuo, A. Faust, H. Zen, and I. Gur. Geometric-averaged preference optimization for soft preference labels. *arXiv preprint arXiv:2409.06691*, 2024.
- Gemini Team. Gemini: A family of highly capable multimodal models. *arXiv preprint arXiv:2312.11805*, 2023.
- R. Goyal, S. E. Kahou, V. Michalski, J. Materzyńska, S. Westphal, H. Kim, V. Haenel, I. Freund, P. Yianilos, M. Mueller-Freitag, F. Hoppe, C. Thureau, I. Bax, and R. Memisevic. The "something something" video database for learning and evaluating visual common sense. *arXiv preprint arXiv:1706.04261*, 2017.
- X. He, D. Jiang, G. Zhang, M. Ku, A. Soni, S. Siu, H. Chen, A. Chandra, Z. Jiang, A. Arulraj, K. Wang, Q. D. Do, Y. Ni, B. Lyu, Y. Narsupalli, R. Fan, Z. Lyu, Y. Lin, and W. Chen. Videoscore: Building automatic metrics to simulate fine-grained human feedback for video generation. *arXiv preprint arXiv:2406.15252*, 2024.
- J. Ho and T. Salimans. Classifier-free diffusion guidance. *arXiv preprint arXiv:2207.12598*, 2022.
- J. Ho, A. Jain, and P. Abbeel. Denoising diffusion probabilistic models. In *Advances in Neural Information Processing Systems*, volume 33, pages 6840–6851, 2020.
- J. Ho, W. Chan, C. Saharia, J. Whang, R. Gao, A. Gritsenko, D. P. Kingma, B. Poole, M. Norouzi, D. J. Fleet, et al. Imagen video: High definition video generation with diffusion models. *arXiv preprint arXiv:2210.02303*, 2022a.
- J. Ho, T. Salimans, A. Gritsenko, W. Chan, M. Norouzi, and D. J. Fleet. Video diffusion models. *arXiv preprint arXiv:2204.03458*, 2022b.
- J. Hoffmann, S. Borgeaud, A. Mensch, E. Buchatskaya, T. Cai, E. Rutherford, D. d. L. Casas, L. A. Hendricks, J. Welbl, A. Clark, et al. Training compute-optimal large language models. *arXiv preprint arXiv:2203.15556*, 2022.
- W. Hong, M. Ding, W. Zheng, X. Liu, and J. Tang. Cogvideo: Large-scale pretraining for text-to-video generation via transformers. *arXiv preprint arXiv:2205.15868*, 2022.
- Z. Huang, Y. He, J. Yu, F. Zhang, C. Si, Y. Jiang, Y. Zhang, T. Wu, Q. Jin, N. Chanpaisit, Y. Wang, X. Chen, L. Wang, D. Lin, Y. Qiao, and Z. Liu. VBench: Comprehensive benchmark suite for video generative models. In *Proceedings of the IEEE/CVF Conference on Computer Vision and Pattern Recognition*, 2024.
- G. Ilharco, M. Wortsman, R. Wightman, C. Gordon, N. Carlini, R. Taori, A. Dave, V. Shankar, H. Namkoong, J. Miller, H. Hajishirzi, A. Farhadi, and L. Schmidt. Openclip, July 2021. URL <https://doi.org/10.5281/zenodo.5143773>.
- X. Ju, Y. Gao, Z. Zhang, Z. Yuan, X. Wang, A. Zeng, Y. Xiong, Q. Xu, and Y. Shan. Miradata: A large-scale video dataset with long durations and structured captions. *arXiv preprint arXiv:2407.06358*, 2024.
- J. Ke, K. Ye, J. Yu, Y. Wu, P. Milanfar, and F. Yang. Vila: Learning image aesthetics from user comments with vision-language pretraining. In *Proceedings of the IEEE/CVF Conference on Computer Vision and Pattern Recognition*, pages 10041–10051, 2023.
- K. Kim, J. Jeong, M. An, M. Ghavamzadeh, K. D. Dvijotham, J. Shin, and K. Lee. Confidence-aware reward optimization for fine-tuning text-to-image models. In *The Twelfth International Conference on Learning Representations*, 2024.
- S. Kim, J. Shin, Y. Cho, J. Jang, S. Longpre, H. Lee, S. Yun, S. Shin, S. Kim, J. Thorne, et al. Prometheus: Inducing fine-grained evaluation capability in language models. In *The Twelfth International Conference on Learning Representations*, 2023.
- Y. Kirstain, A. Polyak, U. Singer, S. Matiana, J. Penna, and O. Levy. Pick-a-pic: An open dataset of user preferences for text-to-image generation. *arXiv preprint arxiv:2305.01569*, 2023.
- P.-C. Ko, J. Mao, Y. Du, S.-H. Sun, and J. B. Tenenbaum. Learning to act from actionless videos through dense correspondences. *arXiv preprint arXiv:2310.08576*, 2023.

- H. Lee, S. Phatale, H. Mansoor, T. Mesnard, J. Ferret, K. Lu, C. Bishop, E. Hall, V. Carbune, A. Rastogi, and S. Prakash. Rlaif: Scaling reinforcement learning from human feedback with ai feedback. *arXiv preprint arXiv:2309.00267*, 2023a.
- K. Lee, H. Liu, M. Ryu, O. Watkins, Y. Du, C. Boutilier, P. Abbeel, M. Ghavamzadeh, and S. S. Gu. Aligning text-to-image models using human feedback. *arXiv preprint arXiv:2302.12192*, 2023b.
- S. Levine. Reinforcement learning and control as probabilistic inference: Tutorial and review. *arXiv preprint arXiv:1805.00909*, 2018.
- B. Li, Z. Lin, D. Pathak, J. Li, Y. Fei, K. Wu, T. Ling, X. Xia, P. Zhang, G. Neubig, and D. Ramanan. Genai-bench: Evaluating and improving compositional text-to-visual generation. *arXiv preprint arXiv:2406.13743*, 2024a.
- J. Li, W. Feng, T.-J. Fu, X. Wang, S. Basu, W. Chen, and W. Y. Wang. T2v-turbo: Breaking the quality bottleneck of video consistency model with mixed reward feedback. *arXiv preprint arXiv:2405.18750*, 2024b.
- Z. Liang, Y. Yuan, S. Gu, B. Chen, T. Hang, J. Li, and L. Zheng. Step-aware preference optimization: Aligning preference with denoising performance at each step. *arXiv preprint arXiv:2406.04314*, 2024.
- M. Liao, H. Lu, X. Zhang, F. Wan, T. Wang, Y. Zhao, W. Zuo, Q. Ye, and J. Wang. Evaluation of text-to-video generation models: A dynamics perspective. *arXiv preprint arXiv:2407.01094*, 2024.
- Z. Ling, Y. Fang, X. Li, Z. Huang, M. Lee, R. Memisevic, and H. Su. Deductive verification of chain-of-thought reasoning. *Advances in Neural Information Processing Systems*, 36, 2024.
- S. Liu, Z. Ren, S. Gupta, and S. Wang. Physgen: Rigid-body physics-grounded image-to-video generation. In *European Conference on Computer Vision (ECCV)*, 2024.
- Y. Liu, X. Cun, X. Liu, X. Wang, Y. Zhang, H. Chen, Y. Liu, T. Zeng, R. Chan, and Y. Shan. Evalcrafter: Benchmarking and evaluating large video generation models. *arXiv preprint arXiv:2310.11440*, 2023.
- F. Mahdisoltani, G. Berger, W. Gharbieh, D. Fleet, and R. Memisevic. On the effectiveness of task granularity for transfer learning. *arXiv preprint arXiv:1804.09235*, 2018.
- T. Matsushima, H. Furuta, Y. Matsuo, O. Nachum, and S. Gu. Deployment-efficient reinforcement learning via model-based offline optimization. In *International Conference on Learning Representations*, 2021.
- Y. Miao, Y. Zhu, Y. Dong, L. Yu, J. Zhu, and X.-S. Gao. T2vsafetybench: Evaluating the safety of text-to-video generative models. *arXiv preprint arXiv:2407.05965*, 2024.
- S. Na, Y. Kim, and H. Lee. Boost your own human image generation model via direct preference optimization with ai feedback. *arXiv preprint arXiv:2405.20216*, 2024.
- OpenAI. Sora, 2024. URL <https://openai.com/index/sora/>.
- L. Ouyang, J. Wu, X. Jiang, D. Almeida, C. Wainwright, P. Mishkin, C. Zhang, S. Agarwal, K. Slama, A. Ray, et al. Training language models to follow instructions with human feedback. *Advances in neural information processing systems*, 35:27730–27744, 2022.
- X. B. Peng, A. Kumar, G. Zhang, and S. Levine. Advantage-Weighted Regression: Simple and scalable off-policy reinforcement learning. *arXiv preprint arXiv:1910.00177*, 2019.
- J. Peters and S. Schaal. Reinforcement learning by reward-weighted regression for operational space control. In *Proceedings of the 24th international conference on Machine learning*, 2007.
- J. Peters, K. Mülling, and Y. Altun. Relative entropy policy search. In *AAAI Conference on Artificial Intelligence*, 2010.
- M. Prabhudesai, A. Goyal, D. Pathak, and K. Fragkiadaki. Aligning text-to-image diffusion models with reward backpropagation. *arXiv preprint arxiv:2310.03739*, 2023.
- M. Prabhudesai, R. Mendonca, Z. Qin, K. Fragkiadaki, and D. Pathak. Video diffusion alignment via reward gradients. *arXiv preprint arXiv:2407.08737*, 2024.
- Z. Qin, R. Jagerman, K. Hui, H. Zhuang, J. Wu, L. Yan, J. Shen, T. Liu, J. Liu, D. Metzler, et al. Large language models are effective text rankers with pairwise ranking prompting. *arXiv preprint arXiv:2306.17563*, 2023.
- A. Radford, J. W. Kim, C. Hallacy, A. Ramesh, G. Goh, S. Agarwal, G. Sastry, A. Askell, P. Mishkin, J. Clark, G. Krueger, and I. Sutskever. Learning transferable visual models from natural language supervision. *arXiv preprint arXiv:2103.00020*, 2021.

- R. Rafailov, A. Sharma, E. Mitchell, C. D. Manning, S. Ermon, and C. Finn. Direct preference optimization: Your language model is secretly a reward model. In *Thirty-seventh Conference on Neural Information Processing Systems*, 2023.
- J. Rocamonde, V. Montesinos, E. Nava, E. Perez, and D. Lindner. Vision-language models are zero-shot reward models for reinforcement learning. *arXiv preprint arXiv:2310.12921*, 2023.
- J. Schulman, F. Wolski, P. Dhariwal, A. Radford, and O. Klimov. Proximal policy optimization algorithms. *arXiv preprint arXiv:1707.06347*, 2017.
- U. Singer, A. Polyak, T. Hayes, X. Yin, J. An, S. Zhang, Q. Hu, H. Yang, O. Ashual, O. Gafni, et al. Make-a-video: Text-to-video generation without text-video data. *arXiv preprint arXiv:2209.14792*, 2022.
- J. Sohl-Dickstein, E. Weiss, N. Maheswaranathan, and S. Ganguli. Deep unsupervised learning using nonequilibrium thermodynamics. In *Proceedings of the 32nd International Conference on Machine Learning*, volume 37, pages 2256–2265, 2015.
- F. Tajwar, A. Singh, A. Sharma, R. Rafailov, J. Schneider, T. Xie, S. Ermon, C. Finn, and A. Kumar. Preference fine-tuning of llms should leverage suboptimal, on-policy data. *arXiv preprint arXiv:2404.14367*, 2024.
- Z. Teed and J. Deng. Raft: Recurrent all-pairs field transforms for optical flow. *arXiv preprint arXiv:2003.12039*, 2020.
- M. Uehara, Y. Zhao, K. Black, E. Hajiramezani, G. Scalia, N. L. Diamant, A. M. Tseng, T. Biancalani, and S. Levine. Fine-tuning of continuous-time diffusion models as entropy-regularized control. *arXiv preprint arXiv:2402.15194*, 2024.
- D. Venuto, S. N. Islam, M. Klissarov, D. Precup, S. Yang, and A. Anand. Code as reward: Empowering reinforcement learning with vlms. *arXiv preprint arXiv:2402.04764*, 2024.
- B. Wallace, M. Dang, R. Rafailov, L. Zhou, A. Lou, S. Purushwalkam, S. Ermon, C. Xiong, S. Joty, and N. Naik. Diffusion model alignment using direct preference optimization. *arXiv preprint arXiv:2311.12908*, 2023.
- H. Wang, S. Pirk, E. Yumer, V. G. Kim, O. Sener, S. Sridhar, and L. J. Guibas. Learning a generative model for multi-step human-object interactions from videos. In *Computer Graphics Forum*, volume 38, pages 367–378. Wiley Online Library, 2019.
- J. Wang, H. Yuan, D. Chen, Y. Zhang, X. Wang, and S. Zhang. Modelscope text-to-video technical report. *arXiv preprint arXiv:2308.06571*, 2023.
- Z. Wang, A. Li, L. Zhu, Y. Guo, Q. Dou, and Z. Li. Customvideo: Customizing text-to-video generation with multiple subjects. *arXiv preprint arXiv:2401.09962*, 2024.
- Z. J. Wang, E. Montoya, D. Munechika, H. Yang, B. Hoover, and D. H. Chau. DiffusionDB: A large-scale prompt gallery dataset for text-to-image generative models. *arXiv preprint arXiv:2210.14896*, 2022.
- J. Z. Wu, G. Fang, H. Wu, X. Wang, Y. Ge, X. Cun, D. J. Zhang, J.-W. Liu, Y. Gu, R. Zhao, W. Lin, W. Hsu, Y. Shan, and M. Z. Shou. Towards a better metric for text-to-video generation. *arXiv preprint arXiv:2401.07781*, 2024a.
- X. Wu, Y. Hao, K. Sun, Y. Chen, F. Zhu, R. Zhao, and H. Li. Human preference score v2: A solid benchmark for evaluating human preferences of text-to-image synthesis. *arXiv preprint arXiv:2306.09341*, 2023a.
- X. Wu, K. Sun, F. Zhu, R. Zhao, and H. Li. Better aligning text-to-image models with human preference. *arXiv preprint arXiv:2303.14420*, 2023b.
- X. Wu, S. Huang, G. Wang, J. Xiong, and F. Wei. Boosting text-to-video generative model with MLLMs feedback. In *The Thirty-eighth Annual Conference on Neural Information Processing Systems*, 2024b.
- X. Wu, S. Huang, and F. Wei. Multimodal large language model is a human-aligned annotator for text-to-image generation. *arXiv preprint arXiv:2404.15100*, 2024c.
- J. Xu, A. Lee, S. Sukhbaatar, and J. Weston. Some things are more cringe than others: Iterative preference optimization with the pairwise cringe loss. *arXiv preprint arXiv:2312.16682*, 2023a.
- J. Xu, X. Liu, Y. Wu, Y. Tong, Q. Li, M. Ding, J. Tang, and Y. Dong. Imagereward: Learning and evaluating human preferences for text-to-image generation. In *Thirty-seventh Conference on Neural Information Processing Systems*, 2023b.
- S. Yan, M. Bai, W. Chen, X. Zhou, Q. Huang, and L. E. Li. Vigor: Improving visual grounding of large vision language models with fine-grained reward modeling. *arXiv preprint arXiv:2402.06118*, 2024.

- K. Yang, J. Tao, J. Lyu, C. Ge, J. Chen, Q. Li, W. Shen, X. Zhu, and X. Li. Using human feedback to fine-tune diffusion models without any reward model. *arXiv preprint arXiv:2311.13231*, 2023a.
- M. Yang, Y. Du, K. Ghasemipour, J. Tompson, D. Schuurmans, and P. Abbeel. Learning interactive real-world simulators. *arXiv preprint arXiv:2310.06114*, 2023b.
- S. Yang, J. Walker, J. Parker-Holder, Y. Du, J. Bruce, A. Barreto, P. Abbeel, and D. Schuurmans. Video as the new language for real-world decision making. *arXiv preprint arXiv:2402.17139*, 2024.
- H. Yuan, S. Zhang, X. Wang, Y. Wei, T. Feng, Y. Pan, Y. Zhang, Z. Liu, S. Albanie, and D. Ni. Instructvideo: Instructing video diffusion models with human feedback. *arXiv preprint arXiv:2312.12490*, 2023.
- H. Yuan, Z. Chen, K. Ji, and Q. Gu. Self-play fine-tuning of diffusion models for text-to-image generation. *arXiv preprint arXiv:2402.10210*, 2024.
- L. Zhang, A. Hosseini, H. Bansal, M. Kazemi, A. Kumar, and R. Agarwal. Generative verifiers: Reward modeling as next-token prediction. *arXiv preprint arXiv:2408.15240*, 2024a.
- Y. Zhang, E. Tzeng, Y. Du, and D. Kislyuk. Large-scale reinforcement learning for diffusion models. *arXiv preprint arXiv:2401.12244*, 2024b.
- Z. Zhang, S. Zhang, Y. Zhan, Y. Luo, Y. Wen, and D. Tao. Confronting reward overoptimization for diffusion models: A perspective of inductive and primacy biases. In *Forty-first International Conference on Machine Learning*, 2024c.
- L. Zheng, W.-L. Chiang, Y. Sheng, S. Zhuang, Z. Wu, Y. Zhuang, Z. Lin, Z. Li, D. Li, E. Xing, et al. Judging llm-as-a-judge with mt-bench and chatbot arena. *Advances in Neural Information Processing Systems*, 36, 2024a.
- Z. Zheng, X. Peng, T. Yang, C. Shen, S. Li, H. Liu, Y. Zhou, T. Li, and Y. You. Open-sora: Democratizing efficient video production for all, March 2024b. URL <https://github.com/hpcaitech/Open-Sora>.
- J. Zhu, H. Yang, H. He, W. Wang, Z. Tuo, W.-H. Cheng, L. Gao, J. Song, and J. Fu. Moviefactory: Automatic movie creation from text using large generative models for language and images. In *Proceedings of the 31st ACM International Conference on Multimedia*, pages 9313–9319, 2023.
- Özgün Çiçek, A. Abdulkadir, S. S. Lienkamp, T. Brox, and O. Ronneberger. 3d u-net: Learning dense volumetric segmentation from sparse annotation. *arXiv preprint arXiv:1606.06650*, 2016.

Appendix

A. Prompts for Challenging Object Movements

Object Removal (Train)

1. digging key out of sand
2. opening a drawer
3. putting coca cola bottle onto johnsons baby oil bottle so it falls down
4. removing beetroot , revealing cauliflower piece behind
5. uncovering pencil
6. wiping foam soap off of cutting board
7. burying flower in leaves
8. closing a bowl
9. plugging airwick scented oil diffuser into plugging outlet but pulling it right out as you remove your hand
10. burying a flower in sand
11. digging a leaf out of sand
12. showing that clip box is empty
13. pulling crucifix from behind of vr box
14. stuffing a ticket into a wooden box
15. taking seisor out of tin
16. glassess falling like a rock
17. rolling pen on a flat surface
18. uncovering a key
19. stuffing key into cup
20. removing red bulb , revealing blue marble behind
21. digging remote control out of sand
22. taking a pen out of the book
23. tilting wooden box with car key on it until it falls off
24. burying tomato in blanket

Object Removal (Test)

1. taking cellphone out of white bowl
2. taking rose bud from bush
3. taking paper out of cigarette can
4. closing box
5. stuffing a bottle opener into a drawer
6. taking gas lighter out of cigarette can
7. scooping banana juice up with spoon
8. taking one of many coins

Multiple Objects (Train)

1. lifting phone with pen on it
2. putting six markers onto a plate
3. putting cellphone , usb flashdisk and gas lighter on the table
4. putting 3 pencil onto towel
5. putting 4 blocks onto styrofoam sheet
6. moving cup and tin closer to each other
7. pushing calculator with marker pen
8. moving a candle and another candle away from each other
9. putting 4 pencils onto blanket
10. moving cup and fork away from each other
11. pushing avacado with book
12. putting a box , a pencil and a key chain on the table
13. moving a glass and a glass closer to each other
14. stacking three legos
15. moving mouse and brush away from each other

16. putting marker pen on the edge of plastic water cup so it is not supported and falls down
17. putting 4 pens onto a paper
18. moving plastic box and plastic box so they pass each other
19. stacking 4 numbers of cassette
20. pretending to close water tap without actually closing it
21. failing to put a drumstick into a purse because a drumstick does not fit
22. putting three shot glasses onto a box
23. taking one body spray of many similar
24. piling chilli up

Multiple Objects (Test)

1. moving coin and napkin away from each other
2. moving lego away from mouse
3. putting lighter into shoe
4. putting spoon and flower on the table
5. attaching lid to sketch pen
6. putting cello tape onto powder container so it falls down
7. moving tv tuner and orange closer to each other
8. putting coins into bowl

Deformable Object (Train)

1. folding cloth
2. folding a rag
3. tearing paper into two pieces
4. twisting (wringing) shirt wet until water comes out
5. tearing receipt into two pieces
6. moving adhesive tape down
7. folding a short
8. unfolding purse
9. tearing paper into two pieces
10. squeezing paper
11. folding paper
12. unfolding cloth
13. tearing tissues into two pieces
14. ziplock bag falling like a feather or paper
15. tearing a piece of paper into two pieces
16. unfolding floor mat
17. unfolding newspaper
18. squeezing toothpaste
19. tearing a leaf into two pieces
20. tearing paper just a little bit
21. spreading leaves onto floor
22. folding letter
23. squeezing a nylon bag

Deformable Objects (Test)

1. tearing paper into two pieces
2. unfolding dish towel
3. unfolding a piece of paper
4. covering glue stick with tissue
5. unfolding blouse
6. stuffing a sock into a jar
7. attaching a cotton swab to paper clip
8. stacking three dish rags
9. folding winter cap

Directional Movement (Train)

1. pulling charger from right to left
2. pushing glove from left to right
3. pulling a tissue box from right to left
4. moving banana away from the camera
5. pushing cup from left to right
6. turning a calculator upside down
7. laying spray bottle on the table on its side , not upright
8. turning makeup product upside down
9. pulling trigonal clip from left to right
10. pushing newspaper from right to left
11. pulling scissors from right to left
12. putting a glass upright on the table
13. pushing glasses from right to left
14. pushing calculator from left to right
15. pushing brush from left to right
16. moving pencil across a surface without it falling down
17. pulling fork from right to left
18. pushing brush from left to right
19. pulling water bottle from left to right
20. pulling fabric from left to right
21. pulling ticket from left to right
22. turning container upside down
23. laying beer bottle on the table on its side , not upright
24. dropping wallet behind flower vase

Directional Movement (Test)

1. pulling a paper bag from right to left
2. pushing rubik ' s cube from right to left
3. pulling a mug from right to left
4. moving cellphone and fork so they pass each other
5. pushing screwdriver from right to left
6. pretending to close a book without actually closing it
7. dropping a battery in front of a teddy bear
8. pushing calculator from left to right

Falling Down (Train)

1. putting marker pen onto plastic bottle so it falls down
2. putting spoon on the edge of glass bottle so it is not supported and falls down
3. pushing a bottle so that it falls off the table
4. pushing key onto basket
5. pushing pocket notebook so that it falls off the table
6. pushing a flashlight so that it falls off the table
7. dropping dumbbell in front of basket
8. dropping toy duck next to teddy bear
9. big book falling like a rock
10. pulling plastic bowl onto floor
11. picking a watch up
12. throwing flask
13. tilting box with tube on it until it falls off
14. putting fork onto candle so it falls down
15. putting foil casserole dish upright on the table , so it falls on its side
16. dropping a ball in front of a book
17. tilting wooden scale with scissor on it until it falls off
18. tipping spray paint can with cap over , so cap falls out
19. moving belt across a surface until it falls down
20. poking an apple so that it falls over

21. lifting yellow marker up completely , then letting it drop down
22. poking menu card so that it falls over
23. tilting tray with buscuit on it until it falls off
24. dropping toothbrush onto stool

Falling Down (Test)

1. pouring beer into glass
2. spilling water next to a plastic bottle
3. lifting a surface with a pawn on it until it starts sliding down
4. tilting smartphone backcover with cough syrup on it until it falls off
5. pushing digital multimeter so that it falls off the table
6. pushing a purse off of an ottoman
7. letting spray paint can roll down a slanted surface
8. poking a stack of books so the stack collapses

B. Prompt for AI Feedback from VLMs

Task: You are a video reviewer evaluating a sequence of actions presented as eight consecutive images in the video below. You are going to accept the video if it completes the task and the video is consistent without glitches.

Inputs Provided:

Textual Prompt: Describes the task the video should accomplish.

Sequence of Images (8 Frames): Represents consecutive moments in the video to be evaluated.

Evaluation Process:

View and Analyze Each Frame: Examine each of the eight images in sequence to understand the progression and continuity of actions.

Assess Overall Coherence: Consider the sequence as a continuous scene to determine if the actions smoothly transition from one image to the next, maintaining logical progression.

Check for Physical Accuracy: Ensure each frame adheres to the laws of physics, looking for any discrepancies in movement or positioning.

Verify Task Completion: Check if the sequence collectively accomplishes the task described in the textual prompt.

Identify Inconsistencies: Look for inconsistencies in object movement or overlaps that do not match the fixed scene elements shown in the first frame.

Evaluation Criteria:

Accept the sequence if it is as a coherent video which completes the task.

Reject the sequence if any frame fails to meet the criteria, showing inconsistencies or not achieving the task. Reject even if there are the slightest errors. Do not be too strict in accepting the videos.

Response Requirement:

Provide a single-word answer: Accept or Reject. Do not give reasoning.

Textual Prompt: {instruction}

Video: {video_tokens}

C. Pseudo Algorithm for RL-Finetuning from Feedback

Algorithm 1 Offline RL-Finetuning Text-to-Video Models with Feedback

- Input:** text-to-video model p_θ , dataset for pre-training $D_{\text{pre}} = \{\mathbf{x}_0^{(i)}, \mathbf{c}^i\}_{i=1}^N$, a set of conditional features for finetuning $C_{\text{fine}} = \{\mathbf{c}^j\}_{j=1}^M$, reward model $r(\mathbf{x}_0, \mathbf{c})$
- 1: Pre-train text-to-video model $p_{\text{pre}}(\mathbf{x}_0 | \mathbf{c})$ with D_{pre} by minimizing $\mathcal{J}_{\text{DDPM}}$
 - 2: Generate video $\hat{\mathbf{x}}_0^j \sim p_{\text{pre}}(\cdot | \mathbf{c}^j)$ conditioned on $\mathbf{c}^j \in C_{\text{fine}}$ to collect dataset for finetuning D_{fine}
 - 3: Label AI feedback $r(\hat{\mathbf{x}}_0^j, \mathbf{c}^j)$ to D_{fine} with VLMs (or metric-based reward such as CLIP)
 - 4: (for RWR) Minimize $\mathcal{J}_{\text{f-EM}}$ (Equation 6) with D_{fine}
 - 5: (for DPO) Minimize $\mathcal{J}_{\text{r-BT}}$ (Equation 8) with a paired dataset from D_{fine}
-

D. Extended Related Works

AI Feedback for LLMs. A wide set of work has explored leveraging AI feedback generated by LLMs to further improve or align generations of the same or a different LLM (Agarwal et al., 2024; Bai et al., 2022; Kim et al., 2023; Ling et al., 2024; Zheng et al., 2024a). There has also been recent work on extracting reward information from VLMs (Rocamonde et al., 2023; Venuto et al., 2024; Yan et al., 2024). Different from them, we explore the ability of long-context VLMs, such as Gemini-1.5 (Gemini Team, 2023), to provide feedback on various aspects of generated videos such as physical plausibility, consistency, and instruction following.

E. Takeaways for Algorithm Choices

Compared to feedback choices, where AI feedback from VLMs is the best among other metric-based rewards, algorithm choices have both positive and negative aspects. In this section, we highlight the takeaways and recommendations for algorithmic designs to help the practitioners.

Forward-EM-Projection. As shown on [Figure 6](#), iterative RWR can continually improve the AI preference, while reverse-BT-projection gets saturated. This is appealing to further scale up the method. In addition, even in offline finetuning, RWR is good at optimizing a metric within a specific set of prompts used for training, as in [Table 2](#), which can happen in a practical use case. On the other hand, this also means that RWR exhibits overfitting in offline finetuning. In case we need to consider the generalization, we may not recommend to use it in an offline manner.

Reverse-BT-Projection. Offline DPO can improve any metric better than forward-EM-projection ([Table 2](#)). Because there is a negative gradient term in the derivative of objective ([Equation 8](#)) such as $\nabla_{\theta} \mathcal{J}_{\text{r-BT-neg}} = \beta \mathbb{E} \left[\left(1 - \sigma \left(\beta \log \frac{p_{\theta}(\mathbf{x}_0^{(1)} | \mathbf{c}) p_{\text{ref}}(\mathbf{x}_0^{(2)} | \mathbf{c})}{p_{\text{ref}}(\mathbf{x}_0^{(1)} | \mathbf{c}) p_{\theta}(\mathbf{x}_0^{(2)} | \mathbf{c})} \right) \right) \nabla_{\theta} \log p_{\theta}(\mathbf{x}_0^{(2)} | \mathbf{c}) \right]$, where $\mathbf{x}_0^{(1)} > \mathbf{x}_0^{(2)}$, reverse-BT-projection can effectively push down the likelihood of undesirable generations. In contrast, [Figure 5](#) demonstrates that DPO with metric-based reward often falls into the over-optimization, where the metrics are improving while the generated videos are visually worsened to the humans. Moreover, the performance of iterative finetuning gets saturated soon ([Figure 6](#)). This is probably because the paired data from one-iteration DPO becomes equally good due to the overall improvement; it is hard and noisy to assign binary preferences correctly.

Summary. Our suggestion is that, in case you are only allowed to access a single offline dataset, or in case you are interested in optimizing metric-based feedback, reverse-BT-projection such as DPO can be a first choice, and in case you have a budget to iterate the process several times, or in case you are interested in optimizing a metric within a specific set of prompts (not considering the generalization), it is worth employing forward-EM-projection such as RWR.

F. Example of Generated Video

In addition to Figure 4, we provide examples of generated videos from pre-trained models, RWR-AIF, and DPO-AIF in Figure 9.



Figure 9 | Generated videos from pre-trained models, RWR-AIF, and DPO-AIF.

G. Failure Mode of Dynamic Scene Generation

We show the failure generations after RL-finetuning in [Figure 10](#), where the text-to-video models still suffer from modeling multi-step interactions (*stuffing a bottle opener into a drawer*), appearance of new objects (*putting 4 pencils onto blanket* and *unfolding purse*), and spatial three-dimensional relationship (*dropping wallet behind flower vase* and *tilting box with tube on it until it falls off*).

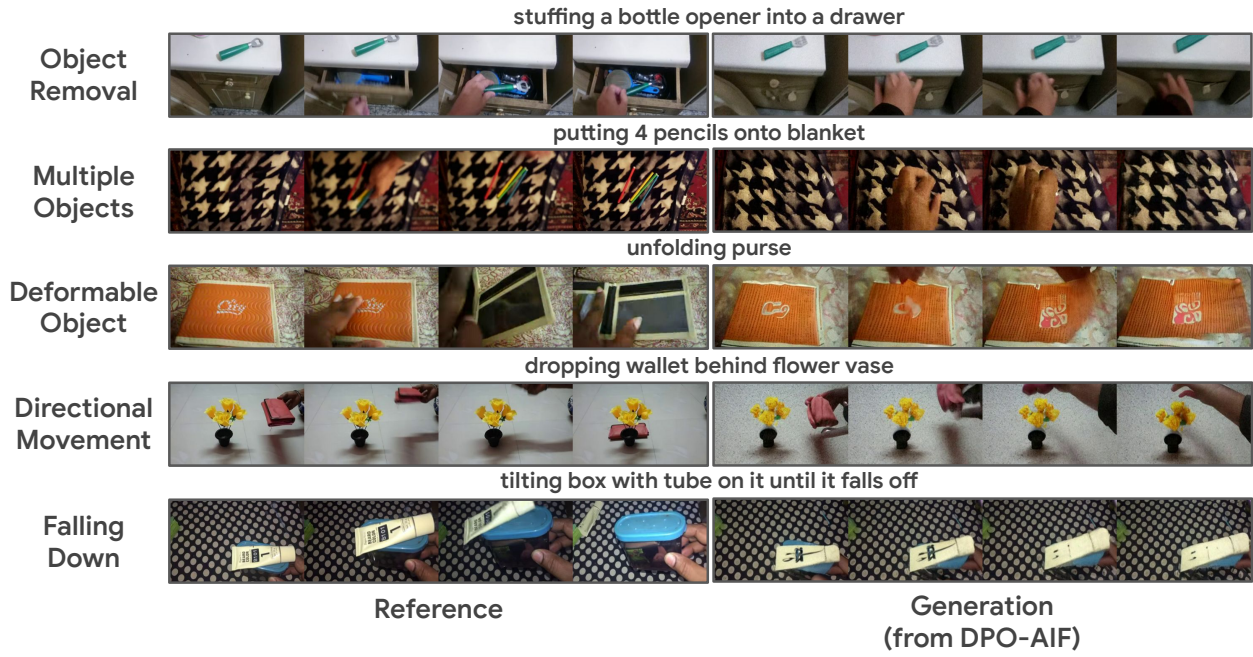


Figure 10 | Failure generations after RL-finetuning. As presented above, the text-to-video models suffer from modeling multiple interactions, appearance of new objects, and spatial three-dimensional relationship.